

# Low Frequency Transport Measurements in $\text{GdSr}_2\text{RuCu}_2\text{O}_8$

A. Vecchione, D. Zola, G. Carapella,\* M. Gombos, S. Pace, G. Costabile, and C. Noce

*Departement of Physics “E. R. Caianiello”, and INFM Research Unit,  
University of Salerno, via S. Allende, I-84081 Baronissi, Italy.*

(Dated: November 7, 2018)

Low frequency transport measurements are performed on  $\text{GdSr}_2\text{RuCu}_2\text{O}_8$  pellets. The observed current-voltage curves are qualitatively explained in the framework of a simple phenomenological model accounting for coexistence of ferromagnetism and superconductivity in the sample. A Curie temperature  $T_{cM}=133$  K and a superconducting critical temperature  $T_{cS}=18$  K, with an onset temperature  $T_{cO}=33$  K, are extracted from the analysis of the current-voltage curves.

## I. INTRODUCTION

The interplay of magnetism and superconductivity is a fundamental problem in condensed-matter physics and it has been studied experimentally and theoretically for almost four decades. These two cooperative phenomena are mutually antagonists. Indeed, the superconductivity is associated with the pairing of electrons states related to time reversal while in the magnetic states the time-reversal symmetry is lost and therefore there is a strong competition with superconductivity<sup>1</sup>. However, Schlabbitz *et al.*<sup>2</sup> showed that surprisingly magnetism and superconductivity could coexist in the heavy fermion compound  $\text{URu}_2\text{Si}_2$ . Other heavy fermion superconductors have also been shown to exhibit magnetic moments in their superconducting phase<sup>3</sup>. All these compounds contain rare-earth or actinide ions with very localized 4f or 5f orbitals, strongly interacting with the conduction band electrons. This is in contrast to the Chevrel phases where magnetism and superconductivity coexist because the magnetic moments responsible for magnetism are only very weakly coupled with the electrons that form the condensate<sup>4</sup>.

Nevertheless, there are been a number of recent studies reporting the coexistence of superconductivity and magnetic order in  $\text{R}_{1.4}\text{Ce}_{0.6}\text{Sr}_2\text{RuCu}_2\text{O}_{10-\delta}$ <sup>5</sup> and  $\text{RSr}_2\text{RuCu}_2\text{O}_8$ <sup>6,7,8</sup> where  $\text{R}=\text{Gd}, \text{Eu}$ . These latter compounds were originally synthesized by Bauernfeind *et al.*<sup>9</sup> and Felner and co-workers<sup>10</sup>. Most recent reports have focused on  $\text{GdSr}_2\text{RuCu}_2\text{O}_8$ , which has a unit cell similar to that of the  $\text{YBa}_2\text{Cu}_3\text{O}_7$  high temperature cuprate, where there are two  $\text{CuO}_2$  layers and one  $\text{RuO}_2$  layer with the  $\text{CuO}_2$  and  $\text{RuO}_2$  layers being separated by insulating layers. Magnetization and muon spin rotation studies<sup>7</sup> have shown that there exists a magnetic ordering transition at temperature much greater than the superconducting transition temperature. Some studies have been interpreted in terms of ferromagnetic order arising from the Ru moment in the  $\text{RuO}_2$  layers. This idea has generated considerable interest because ferromagnetic order and superconductivity are mutually competing processes and could only coexist via some accommodation of the respective order parameters by a spatial modulation<sup>11</sup> or via the formation of a spontaneous vortex phase<sup>12</sup>. However, powder neutron diffraction study<sup>13</sup> has shown

that while there is a small ferromagnetic component, the low-field magnetic order is predominantly antiferromagnetic. These contrasting reports cast some doubt about the magnetic nature of this compound and at the present the situation has not been completely clarified. The aim of this paper is to give a contribution to this discussion. Indeed, we have found that transport measurements performed on  $\text{GdSr}_2\text{RuCu}_2\text{O}_8$  sample are in agreement with predictions of a simple phenomenological model where *ferromagnetism* and superconductivity coexist. From the experimental results a Curie temperature  $T_{cM}=133\text{K}$  and a superconducting critical temperature  $T_{cS}=18\text{K}$ , with an onset temperature  $T_{cO}=33\text{K}$ , have been inferred. The paper is organized as follows. In Section II the sample preparation is discussed. A phenomenological model for expected current-voltage curves is then given in Section III. Experimental results are presented and discussed in connection with the theoretical prediction of the proposed model in Section IV. Some conclusions are finally given in the last Section.

## II. SAMPLE PREPARATION AND CHARACTERIZATION

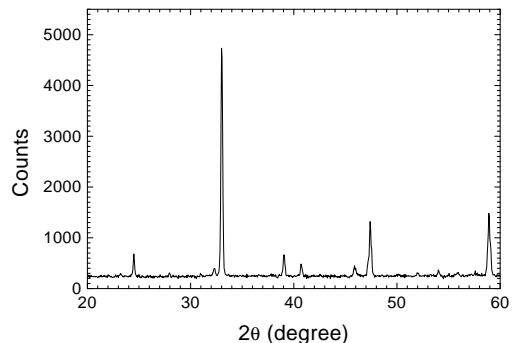


FIG. 1: (a) X-ray diffraction patterns of the  $\text{GdSr}_2\text{RuCu}_2\text{O}_8$ .

Precursors powders have been synthesized starting from the pure binary oxide and carbonate powders,  $\text{Gd}_2\text{O}_3$ ,  $\text{SrCO}_3$ ,  $\text{CuO}$ , and  $\text{RuO}_2$ , mixed together in the proper amount and solid state reacted. The mixed pow-

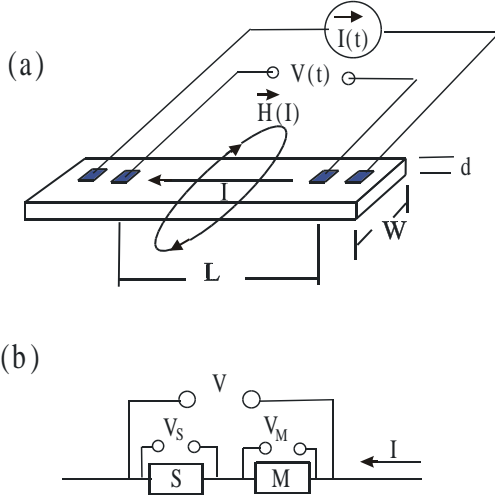


FIG. 2: (a) Sketch of wire connections used to measure a  $\text{GdSr}_2\text{RuCu}_2\text{O}_8$  pellet. (b) Measured voltage is assumed to be the sum of two contributions.  $V_M$  is associated to the magnetic phase and  $V_S$  to the superconductive (or normal) phase.

der was calcinated in air at  $960^\circ\text{C}$  for 10 h. Annealing in flowing pure nitrogen at  $1000^\circ\text{C}$  during 10 h was performed to reduce the formation of undesired phases such as  $\text{SrRuO}_3$ <sup>9</sup>. Additional two steps of annealing of 10 h pure flowing argon at  $1020^\circ\text{C}$  also contributed to suppress the  $\text{SrRuO}_3$  phase. Subsequently, the powders were oxygenated. Seven oxygenation cycles of a mean duration of 10 h, were performed at  $1060^\circ\text{C}$  in flowing pure oxygen. These fully oxygenated powders were pressed in pellets by means of an hydrostatic press. Five 10 h cycles in pure oxygen flux, at temperatures of  $1050^\circ\text{C}$ ,  $1055^\circ\text{C}$ ,  $1060^\circ\text{C}$ ,  $1065^\circ\text{C}$ , and  $1070^\circ\text{C}$ , with intermediate grinding and mixing, have been performed on the pellets. Then, a last 90 h long cycle at  $1070^\circ\text{C}$  and a refining one of 10 h at  $1065^\circ\text{C}$  assured the complete oxygenation of the pellets. The crystal structure of the  $\text{GdSr}_2\text{RuCu}_2\text{O}_8$  pellets was analyzed by X-ray powder diffraction method. The data were collected with a Philips PW-1700 powder diffractometer using Ni-filtered  $\text{Cu K}\alpha$  radiation. The X-ray spectrum of a typical fully oxygenated pellet is shown in Fig. 1. The scan pattern confirms that the sample is  $\text{GdSr}_2\text{RuCu}_2\text{O}_8$  single phased.

### III. EXPECTED AC CURRENT-VOLTAGE CURVES

If a magnetic phase is present in the  $\text{GdSr}_2\text{RuCu}_2\text{O}_8$ , an hysteretic current-voltage ( $I-V$ ) curve should be expected when the current is swept with a frequency  $\omega$ . In transport measurements, the four contact wire connection sketched in Fig. 2(a) is typically used. Here, the forcing

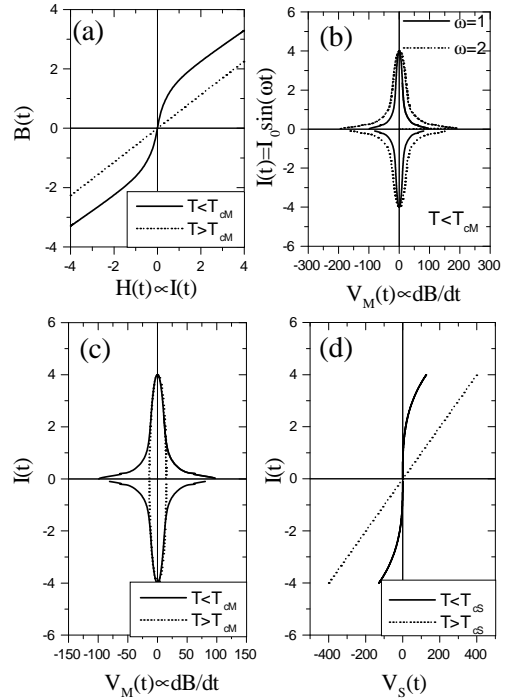


FIG. 3: (a) Low magnetic field approximation of  $B(H)$  for the ferromagnetic phase ( $T < T_{cM}$ ) and the paramagnetic phase ( $T > T_{cM}$ ). (b)  $I-V_M$  curves of the ferromagnetic phase for two different pulsations of a sinusoidal current forcing. (c) The shape of ac  $I-V_M$  curves is truly elliptical for the paramagnetic phase and becomes a distorted ellipse in the ferromagnetic phase. (d) Typical  $I-V_S$  curves of the superconductive ( $T < T_{cS}$ ) or resistive ( $T > T_{cS}$ ) phases.

ing current  $I(t)$  generates a magnetic field  $\mathbf{H}(t)=\mathbf{H}[I(t)]$  with an associated magnetic induction  $\mathbf{B}(t)=\mathbf{B}[\mathbf{H}(t)]$ . To the first order, the magnetic field depends linearly on the forcing current,  $H(t) \propto I(t)$ , so that  $B(t) = B[I(t)]$  is too. From Maxwell equations, we expect a voltage drop contribution due to the temporal derivative of the magnetic flux linked to the voltage wires. However, such a contribution is quite relevant only if the magnetic induction field is quite high, i.e., if magnetic phases are involved. The  $\text{GdSr}_2\text{RuCu}_2\text{O}_8$  can be phenomenologically seen as a series connection of superconducting and magnetic phases. Hence, we expect the measured total voltage to be the sum of a superconducting contribution  $V_S$  and a magnetic contribution  $V_M$  [see Fig. 2(b)]:

$$V = V_S + V_M$$

$$V_M = \frac{d\Phi[B]}{dt} \propto \frac{dB(t)}{dt} = \frac{dB[I(t)]}{dt}$$

where we assumed that the relevant inductive voltage is essentially due to the magnetic component. Some qualitative predictions of the  $I-V_M$  characteristic are possible from an analysis of the expected  $B[I(t)]$ .

Generally,  $\mathbf{B}$  is a nonlinear function of  $\mathbf{H}$  when a material is in a magnetic phase. In the following we are concerned with low magnetic field (forcing current) am-

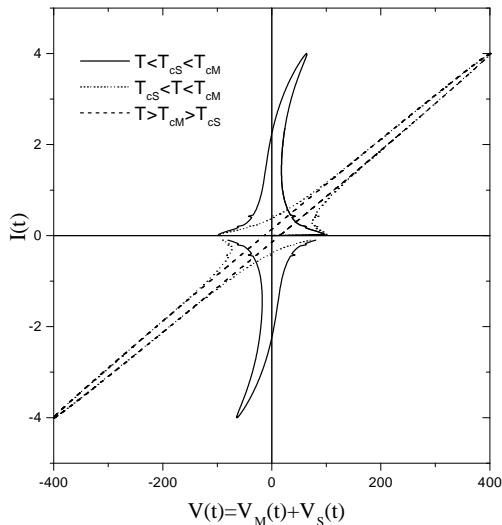


FIG. 4: Total ac current-voltage curve predicted for GdSr<sub>2</sub>RuCu<sub>2</sub>O<sub>8</sub> pellet at three relevant temperatures.

plitudes. In such a case, a linear relationship between  $\mathbf{B}$  and  $\mathbf{H}$  can be assumed for the paramagnetic phase. Due to the vanishingly small net magnetization, for an antiferromagnetic phase an approximately linear  $B(H)$  relation could be again inferred, while a nonlinear relation should be expected for a strongly ordered phase as the ferromagnetic one. The last case can be qualitatively discussed as follows. At a given low amplitude magnetic field, a linear relation between  $\mathbf{B}$  and  $\mathbf{H}$  [see Fig. 3(a)] can be expected for temperatures above the ferromagnetic transition temperature  $T_{CM}$  (i.e., when the material is in the paramagnetic phase) while a strongly nonlinear relation between  $\mathbf{B}$  and  $\mathbf{H}$  should be expected for temperatures below  $T_{CM}$  (i.e., when the material is in the ferromagnetic phase). Due to the very low magnetic fields we can generate with the normally used forcing currents (of the order of some mA) we can assume that the saturation field will never be reached when the material is in the ferromagnetic phase. In other words, for the used currents only the virgin curve of the hysteresis loop will be normally swept, so that a single-valued functional form  $B(t) = B[I(t)]$  similar to the one shown in Fig. 3(a) can be expected to approximately describe the material in the ferromagnetic phase. In such a limit, for a sinusoidal forcing current of amplitude  $I_0$  and pulsation  $\omega$  the  $I - V_M$  curves shown in Fig. 3(b) should be observed for the ferromagnetic phase. Moreover, the distorted ellipse typical of the ferromagnetic phase (at  $T < T_{CM}$ ) should become a pure ellipse in the paramagnetic phase (at  $T > T_{CM}$ ), as shown in Fig. 3(c).

Referring to the superconducting phase, the standard ac  $I - V_S$  curves schematically plotted in Fig. 3(d) are expected for temperatures below or above the superconducting transition temperature  $T_{CS}$ . For  $T < T_{CS}$  is  $V_S = 0$  for amplitude of the forcing current lower than

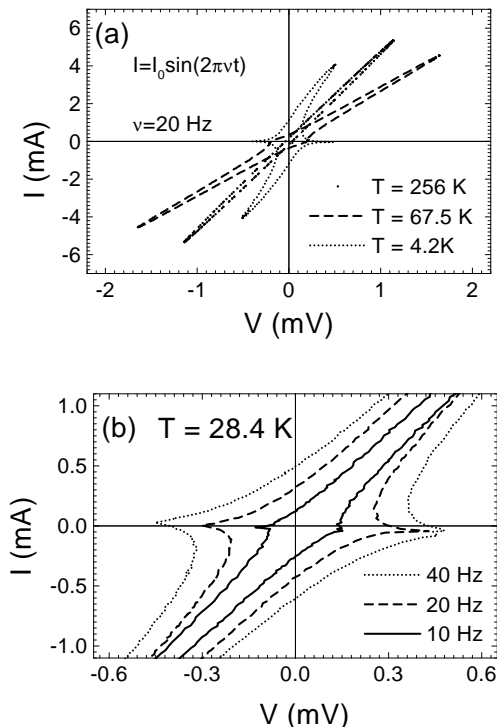


FIG. 5: (a) Experimental  $I - V$  curves measured at three different temperatures. The frequency of current supply was 20 Hz. (b)  $I - V$  curves measured at  $T=28.4$  K at different frequencies

a critical current value  $I_c$ , while a truly resistive curve is observed for  $T > T_{CS}$

As stated above, the measured voltage of GdSr<sub>2</sub>RuCu<sub>2</sub>O<sub>8</sub> pellet is  $V = V_M + V_S$ . Hence, from information in Figs. 3(c) and (d), the expected ac  $I - V$  curves should look similar to the ones we plotted in Fig. 4 for three relevant temperatures.

We should remark that, if observed, the peculiar outward cusp-like distortion of the  $I - V$  curve around  $I = 0$  is a signature of a ferromagnetic order originating from the strong nonlinear increase of the magnetic susceptibility below the Curie temperature. Conversely, for an antiferromagnetic order, a smoother distortion of the  $I - V$  curve should be expected, and the area of the ellipse of the paramagnetic phase should decrease for temperatures below the Neel temperature due to the decrease of the magnetic susceptibility of the antiferromagnetic phase when the temperature is lowered.

#### IV. TRANSPORT MEASUREMENTS AND DISCUSSION

Measurements of  $I - V$  curves were performed on a slice of GdSr<sub>2</sub>RuCu<sub>2</sub>O<sub>8</sub> using the four contact technique shown in Fig. 2(a). The sizes of the slice were  $L=5$  mm,  $W=2$  mm, and  $d=0.7$  mm. A sinusoidal forcing current

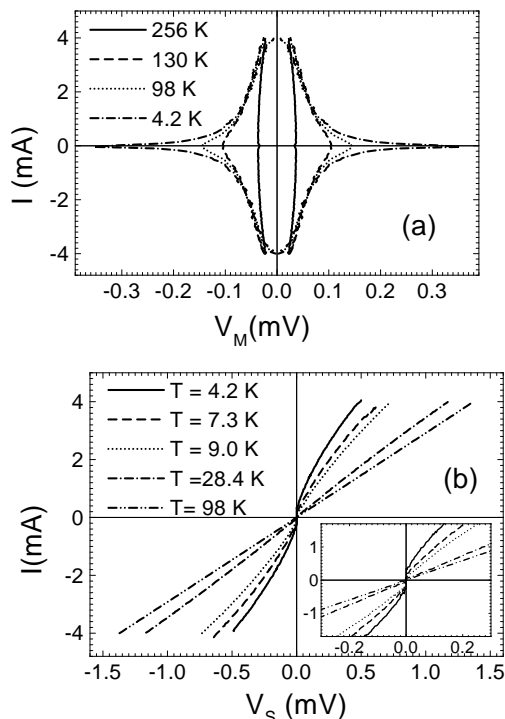


FIG. 6: Irreversible (a) and reversible (b) component extracted by experimental  $I - V$  curves.

ranging from 4 mA to 6 mA and frequency values of 10, 20 and 40 Hz were used. In order to reduce external electromagnetic interference, measurements were performed in a shielded room. The sample was also enclosed in a cryoperm shield to minimize external spurious magnetic field.

In Fig. 5(a),  $I - V$  curves recorded at three different temperatures are shown. At first sight, the curves are in qualitative agreement with the calculated ones [see Fig. 4], resulting from the phenomenological model reported in the previous Section. The  $I - V$  curves show an hysteretic behavior at each temperature measured. Below a certain temperature, an outward cusp-like distortion of the elliptical shape at  $T=256$  K is evident in the curves. Moreover, the loop area always increases when temperature is lowered. As stated in the previous section this means that a *ferromagnetic* phase is involved in the material.

Figure 5(b) shows that the loop area increases with the frequency of the current sweep, as expected for an inductive (magnetic) contribution  $V_M \propto dB/dt$  to the total voltage drop. By comparison of Fig. 5(b) and Fig. 3(b), a voltage contribution from a ferromagnetic phase is achieved. In the previous section, we have assumed that the electrical response of the material can be described as the series connection of a normal (superconducting/resistive) phase and a magnetic (ferromagnetic/paramagnetic) phase. When the material is a.c. supplied, the resistive (normal) component gives a re-

versible voltage signal, whereas the inductive (magnetic) one gives rise to an irreversible response accounting for the hysteretic shape of the voltage-current curves in the  $I - V$  plane. In order to study separately the resistive and the inductive components of the measured  $I - V$  curves, the reversible ( $V_S$ ) and the irreversible ( $V_M$ ) voltage were extracted in each curve. The reversible component in the total voltage signal, was calculated by using the simple formula

$$V_S(I) = \frac{V_{up}(I) + V_{dw}(I)}{2} \quad (1)$$

where  $V_{up}$  and  $V_{dw}$  are respectively the voltage values measured during the increasing and the decreasing branch of the sinusoidal forcing current. Then, the irreversible component was extracted according to

$$V_M(I) = V(I) - V_S(I) \quad (2)$$

The irreversible part extracted from the total signal measured is shown in Fig. 6(a). Again, a qualitative agreement with the computed curves [see Fig. 3(b)] is recognized. For temperatures ranging from 4.2 K up to about 70 K, the loop area diminishes very slowly. Then the area decreases quickly and smoothly changes shape becoming elliptical around  $T_{cM}=133$  K. From analysis of the previous Section we identify  $T_{cM}=133$  K as the Curie transition temperature of the magnetic phase in the sample. In Fig. 6(b) the reversible curves, ascribed to the resistive share in the total voltage signal, are shown for different temperatures. The typical non linear  $I - V$  for a superconductor ( $V_S = 0$  for  $-I_c < I < I_c$ ) can be recognized for temperatures below  $T_{cS}=18$  K while linear behavior is recovered above this temperature.

From data of the reversible curve, we extracted the resistance as a function of the temperature shown in Fig. 7. The temperature  $T_{cS}$ , corresponding to a full superconducting phase in the sample ( $V_S = 0$ ) and the onset temperature  $T_{cO}$  were estimated 18 K and 33 K, respectively. In our measurements the non-linear behavior in reversible  $I - V$  curves, can be recognized up to 18 K. Increasing the temperature from  $T_{cS}$  up to  $T_{cO}$  the reversible  $I - V$  curves are linear with a quite fast increase of the resistivity. Above  $T_{cO}$ , the measured resistance get lower and for  $T_{cM}=133$  K the resistance shows a peak. For temperatures above the magnetic transition temperature the resistance diminishes again.

Two main results can be drawn from the data above presented.

Firstly, we find a clear evidence of changes near 130K of irreversible and reversible components of the  $I - V$  curves and therefore we infer that they could be ascribed to a ferromagnetic/paramagnetic-like transition. This speculation agrees well with the results reported in literature that find a magnetic ordering temperature at around 130K<sup>6</sup>. The appearance of a spontaneous magnetic moment below this temperature at a very low field suggests that the transition at  $T_{cM}$  must have a significant ferromagnetic component. The experimental results

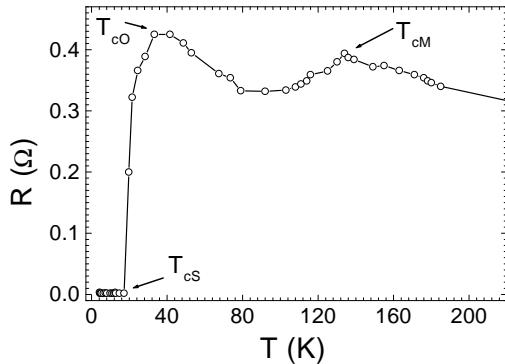


FIG. 7: Resistance versus temperature calculated by using the reversible  $I - V$  curves.

also suggest that the ferromagnetic component persists to the lowest measured temperature attained in the experiments and does not appear to weaken when the superconductivity comes in at  $T_{cO}=33\text{K}$ . The existence of a ferromagnetic component in the superconducting state of this sample suggested by the low frequency data here presented, is also supported by magnetic measurements performed on the same sample and reported elsewhere<sup>14</sup>. Moreover, because no impurity lines were detected in the X-ray diffraction pattern within the experimental resolution we may argue that no extra phases are responsible for ferromagnetism implying that this ordering is due to an intrinsic phase and in this respect we could infer that the coexistence of superconductivity and ferromagnetism is realized within a microscopic scale. This hypothesis is corroborated by magneto-optical-imaging measurements where ferromagnetism and superconductivity are directly observed to coexist in the same space within the experimental resolution<sup>15</sup>.

Second, we speculate briefly on the significance of the

phenomenological model previously introduced. Within our model, we assume that the measured total voltage is the sum of two contributions: one coming from the superconducting channel and the other due to the ferromagnetic ordering. Although the crudeness of the assumptions, we have been able to reproduce fairly the shape of the  $I - V$  curves and more importantly we clearly identify the superconducting contribution only when the ferromagnetic one is subtracted. This contribution is of the standard form for a generic superconductor and this in turn further supports the correctness of our assumptions.

## V. CONCLUSION

In conclusion, we performed measurements on  $\text{GdSr}_2\text{RuCu}_2\text{O}_8$  ruthenate-cuprate with the aim to address the question of the nature of the magnetic order in the superconducting phase and trying to improve the understanding of the physics of ruthenate-cuprate materials. We used a relatively unexplored approach, based on the analysis of low frequency electrical transport measurements. The observed current-voltage curves have been found in quite good qualitative agreement with the predictions of a phenomenological model accounting for coexistence of both magnetic and superconducting phases in the sample. Our experimental results suggest that  $\text{GdSr}_2\text{RuCu}_2\text{O}_8$  is paramagnetic above  $T_{cM}=133\text{ K}$ , ferromagnetic between  $T_{cS}=18\text{ K}$  and  $T_{cM}=133\text{ K}$ , and both ferromagnetic and superconducting below  $T_{cS}=18\text{ K}$ .

## VI. ACKNOWLEDGEMENTS

We gratefully acknowledge the contribution of D. Sisti in the sample preparation.

\* Corresponding author;  
e-mail: giocar@sa.infn.it;  
FAX: +3908965390

<sup>1</sup> M.B. Maple, *Physica B* **215**, 110, (1995).

<sup>2</sup> W. Schlabitz *et al*, *Z. Phys. B: Condens. Matter* **62**, 171 (1986).

<sup>3</sup> A. Amato, *Rev. Mod. Phys.* **69**, 1119, (1997).

<sup>4</sup> O. Fischer, *Appl. Phys.* **16**, 1 (1978).

<sup>5</sup> I. Felner, U. Asaf and O. Millo, *Phys. Rev. B* **55**, R3374 (1997).

<sup>6</sup> J. Tallon *et al.*, *IEEE Trans. Appl. Supercond.* **9**, 1051 (1999).

<sup>7</sup> C. Bernhard *et al.*, *Phys. Rev. B* **59**, 14099 (1999).

<sup>8</sup> G. V. M. Williams, S. Krämer *Phys. Rev. B*, **62**,

4132(2000)).

<sup>9</sup> L. Bauernfeind, W. Widder, and H. F. Braun, *Physica C* **254**, 151 (1995); L. Bauernfeind, W. Widder, and H. F. Braun, *Journ. of Low Temp. Phys.* **105**, 1605 (1996).

<sup>10</sup> I. Felner, U. Asaf, S. Reich, and Y. Tsabba, *Physica C* **311**, 163 (1999).

<sup>11</sup> C. W. Chu *et al*, *Physica C* **335**, 231 (2000).

<sup>12</sup> E. B. Sonin and I. Felner, *Phys. Rev. B* **57**, 14000 (1998); I. Felner, U. Asaf, Y. Levi, and O. Millo, *Physica C* **334**, 141 (2000).

<sup>13</sup> J.W. Lynn *et al.*, *Phys Rev B* **61**, 14 964 (2000).

<sup>14</sup> A. Vecchione *et al.*, *cond-mat/0110482*.

<sup>15</sup> C.W. Chu *et al.*, *cond-mat/9910056*.